

Field investigation on load distribution and deflections of railway track sleepers

Jabbar Ali Zakeri^{1,*} and Javad Sadeghi²

¹Dean of Track Department, Assistant Professor, School of Railway Engineering,

²Assistant Professor, School of Railway Engineering, Iran University of Science and Technology

(Manuscript Received August 6, 2006; Revised June 26, 2007; Accepted July 1, 2007)

Abstract

Despite the significant role of sleepers in railway track mechanical behavior, no thorough mechanistic approach has been presented for the development of the loading pattern they experience. The current theoretical methods in the analysis of the railway track system need further calibration and verification using field-measured data. In this paper, using specific load-cells between sleepers and the rail and beneath the sleepers, the vertical loading conditions of these main track elements are studied. The lateral resistance of the concrete sleepers in the ballasted tracks is investigated by using full scale sleeper pull-out tests. Moreover, track deflections under the sleeper as the main track analysis parameter are measured and the results are discussed. In this paper, with the results obtained from extensive field measurements, some suggestions are made leading to an improvement in the current understanding of the sleeper loading pattern and the track deflections.

Keywords: Sleeper; Loading pattern; Load-cell; Railway track

1. Introduction

Railway sleepers are the main structural elements in the railway track system. As well as pressure distribution and load transfer to the underlying layers, railway sleepers maintain track gauge, guarantee lateral stability of the track and contribute towards providing better track geometry [1]. Vertical, lateral and axial forces are applied to sleepers. These forces are transferred to the underlying soil layers.

A review of the literature indicates that there is a lack of comprehensive experimental investigation into the sleeper-ballast contact pressure and the load transfer mechanism in the track structure [2]. The research presented here is conducted to provide a better understanding of the load transfer mechanism and the resulting deflections of the track. The field

measurements taken in the scope of this research are as follows [3]:

- (1) Evaluation of the vertical and lateral sleeper resistance by the installation of load-cells in the ballast-sleeper interface and between the rail and the sleeper and by the implementation of a sleeper "pull-out" test.
- (2) Investigation of railway track deflections under axle loads.

In this paper the theoretical background of the subject is presented. Test procedures and the test conditions are described. The results are presented and discussed leading to new suggestions and recommendations on the determination of sleeper loading pattern and the calculation of track deflections.

2. Theoretical analysis of sleeper

Current practices in the analysis and design of railway sleepers are based on four main steps [4]. First,

*Corresponding author. Tel.: +98 21 7391 3517, Fax.: +98 21 7745 1568
E-mail address: Zakeri@iust.ac.ir

the wheel loads are considered as static and a dynamic coefficient factor is taken into account to compensate for the effects of the dynamic properties of the loads. Second, the load transferred from the rail to the sleepers is defined as a percentage of the wheel load. Third, a pressure distribution pattern is considered beneath the sleeper. Fourth, the bending moments at the rail seat positions and at the center of the sleeper are calculated, applying an assumed loading pattern. These bending moments then are compared with the allowable bending capacity of the sleeper [5].

Before the sleeper can be analyzed in terms of its capacity to withstand the bending stresses caused by the vertical rail seat loads, the sleeper support conditions and the contact pressure distribution between the sleeper and the ballast must be quantified. There is a dispute over the determination of the load transferred from the rail to the sleepers and the pressure distribution pattern beneath the sleepers. Although there has been considerable theoretical research conducted on the investigation of the railway sleeper analysis, there is a lack of sufficient experimental work and its associated calibration with the theoretical results [2]. A summary of the main theoretical results is presented below.

2.1 Maximum rail-seat load

Maximum rail-seat load depends on several factors such as rail profile and its weight, sleeper distance, track modulus, axial lag between rail and sleepers, axial deformation between sleepers and ballast layer, and track maintenance activities [6]. There are several suggestions made for the determination of the load transferred from the rail to the sleepers. As indicated in Table 1, the rail seat load (q_r) is considered as a percentage of the wheel load (P).

2.2 Sleeper-ballast contact pressure

In a newly tamped ballasted track, contact pressures are mainly concentrated beneath the rail seat. Under accumulated traffic loading, sleeper-pressure

Table 1. Recommended maximum rail-seat loads [2].

Method	Formulas
Three adjacent sleepers	$q_r=0.5P$
BEF (Timer Sleepers), Australia	$q_r=0.43P$
AREMA (Concrete Sleepers), USA	$q_r=0.6P$
UIC (Type F, pre-stressed concrete sleepers), European Countries	$q_r=0.65P$

follows a uniform pattern and results in an increase in the bending moment at the center of the sleeper. Practically, the consideration of a uniform pressure distribution under the sleeper is very dependent on the condition of the ballast and the sleeper. Various hypothetical contact pressure distributions between the sleeper and the ballast are presented in Table 2.

It is most common to assume a uniform pressure distribution along the sleeper-ballast contact area. Thus, the average sleeper-ballast contact pressure (q_r) can be stated as follows.

$$P_r = \left(\frac{P}{B.L} \right) F_2 \tag{1}$$

In which P_r is the average contact pressure (N/m^2), P is the wheel load (N) and B (m) and L (m) are the sleeper width and the effective sleeper length, respectively. F_2 is the safety factor which depends on the sleeper type and track maintenance level. According to AREMA [5], the sleeper effective length (L) is equal to the track gauge length when calculating the bending moment at the center of the sleepers. The sleeper effective length is obtained from the following formula when the bending moment is calculated at the rail seat position of the sleepers.

$$L=l-g \tag{2}$$

Where “ l ” is the total length of the sleeper and “ g ” is the track gauge length. AREMA [5] suggests that the sleeper effective length (L) be equal to the total length of the sleeper when pre-stressed sleepers are analyzed.

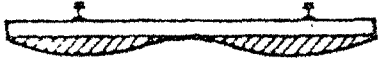

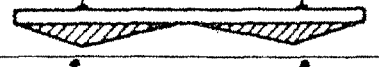
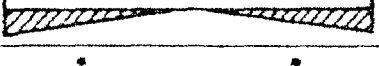

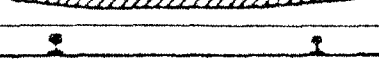
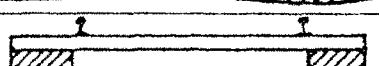
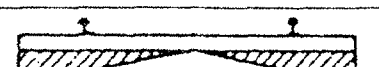
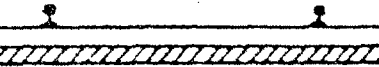
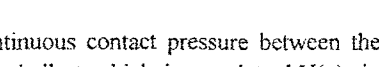
2.3 Sleeper deflection in the track

Currently, the sleeper deflection under the rail is the main criterion in a railway track analysis [7]. It is also a significant factor in track deterioration [8]. The most common method of calculating sleeper deflection (deflection of the rail at the sleeper positions) is the Winkler equation:

$$EI \frac{d^4 y}{dx^4} + p(x) = q(x) \tag{3}$$

Where $y(x)$ is the vertical deflection of the rail at the distance “ x ” from the load point, $q(x)$ is distributed vertical load, EI is the flexural rigidity of the rail,

Table 2. Proposed stress distribution under railway sleepers [2].

Item No.	Proposed Stress Distribution Pattern	Researcher or Standard	Remarks
1		UIC, Talbot	Distribution pattern according to laboratory tests
2		UIC, Talbot, Battelle, Clarke	Tamping effects and ballast compaction in the vicinity of rail
3		UIC, Talbot	Maximum stress under the rail
4		UIC, Talbot	Maximum stress on sleeper sides
5		Talbot	Maximum stress on in the middle of sleeper
6		Talbot	Stress concentration in sleeper center
7		Talbot	Valid for flexible sleepers
8		UIC, Talbot, Kerr, Schramm	Compaction of side ballast and gapping effects in the central ballast
9		UIC, Talbot	Trapezoid distribution
10		AREA, Raymond, Talbot	Uniform stress distribution

$p(x)$ is the continuous contact pressure between the sleeper and the ballast which is equal to $kY(x)$, in which “ k ” is the modulus of the foundation under the sleeper. This equation may be represented as the response of an infinite beam attached to a spring base, subjected to a load $q(x)$. The general equation of the Winkler equation has been developed in detail by Hetenyi [9]. The solution of rail deflection at any distance (x) from the point load is as follows.

$$y_x = \frac{p\beta e^{-\beta x}}{2k} (\cos \beta x + \sin \beta x),$$

$$\beta = \left(\frac{k}{4EI} \right)^{0.25} \quad (4)$$

The beam on an elastic foundation analysis has some limitations when applied to railway track conditions. This model neglects any continuity or coupling of the ballast and subgrade layers which depend on the track foundation. The magnitude of the coupling effect depends on the sleeper spacing, the sleeper size, the ballast depth, and the subgrade properties. There

is no adequate modeling of the stress-strain behavior of the ballast and the subgrade. Thus, the model is of limited value in considering the behavior of the substructure beneath the rail. The simple Winkler model does not include several additional factors which are known to affect the stresses and deflections of the railway track. These include longitudinal loads from thermal stresses, a restoring moment proportional to the rotation of the rail and sleeper, the eccentricity of the vertical load on the rail head and the track dynamic effect from inertial and damping forces. However, despite these deficiencies the Winkler model has been the most common model used in railway track analysis. Its ease of use has been approved, but its degree of accuracy needs further evaluation.

3. Field measurement methodology

A thorough field investigation is conducted in this research. The main objectives of the field tests are to evaluate some of the theoretical analysis results pre-

viously obtained and to provide a better understanding of the load transfer mechanism in the railway track system. The site is located in a suburb of Tehran (the capital city of Iran). The properties of the track in the field are as follows. Rail is UIC60; sleeper is prestressed concrete sleeper type B70; the fastening system is Vossloh. The ballast and sub-ballast thicknesses are 30 and 15 centimeters, respectively. Ballast and sub-ballast aggregates are granite with a size of 40 to 60 mm. The subgrade is well compacted soil ranked $A_{2,7}$ in the AASHTO soil classification.

To evaluate the vertical sleeper resistance, load-cells are installed at the bottom of the sleeper (between the ballast and the sleeper). For evaluating the lateral resistance of sleepers the “Pull-Out” resistance-meter type “K625N” is used. For the evaluation of the deflections of the track, sleeper deformations under the track loads are measured by using a surveying method. More details of the test procedure follow.

3.1 “Load-Cell” application and layout

Fig. 1 indicates the “Load-Cell” layout beneath the

rail seat and between the sleeper and the ballast layer. Considering the working conditions, the capacity and type of “Load-Cells” are selected [3]. For this particular application, 10-ton and 2.5-ton “Load-Cells” were chosen and used at the rail seat position and between the sleeper and the ballast, respectively. Since it is assumed that the sleeper loading pattern is symmetrical, “Load-Cells” were installed only in one half of the sleepers.

Five load-cells with accuracy of 0.0001 were used. One load cell (numbered one) was installed beneath the rail at the rail seat position. Four load cells were installed beneath the half of the sleeper in an equal distance from each other (numbered from 2 to 5). The sleeper with the installed load cells is presented in Fig. 2. Using a “Data logger” and a software package, the output signals from the load-cells are transferred to a computer. The software can obtain data from all load-cells simultaneously and import them into the Excel program. The data-logger and the computer assembly are presented in Fig. 3.

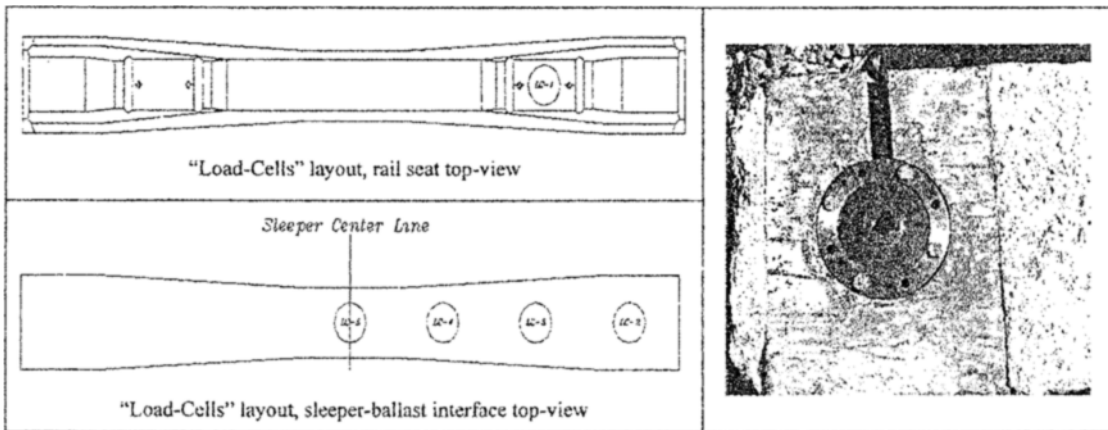


Fig. 1. “Load-Cells” layouts.

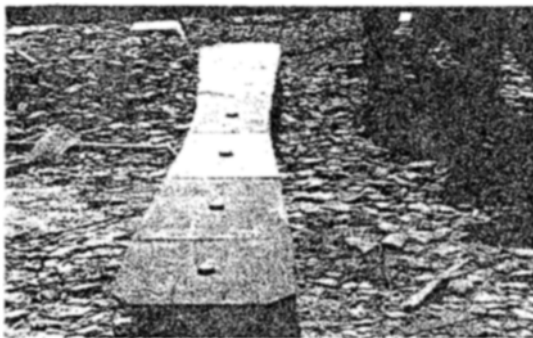


Fig. 2. “Load-Cells” installation underneath sleepers.



Fig. 3. Final assembly (data logger).

3.2 "Pull-Out" test assembly

The Pull-Out test instruments are presented in Fig. 4. These instruments record the lateral resistance of the sleepers for each 0.5 millimeter of lateral movement. This test is applied to the track with compacted ballast under accumulated traffic loading as well as right after the tamping operation. In both conditions, incremental loadings are applied and the load-deformation curves are obtained.

3.3 Surveying method

Since the surveying method provides results with an acceptable level of accuracy, and the surveying cams can be installed at a position far from the track which acts as reference point, a surveying method is used for the measurements of the sleeper deflection under the rail. To record the deflection, a reference point for the installation of the cam was chosen. Some points were marked on the rail just on the top of the sleeper positions, and the first reading was made when the rail was in the no load condition. This was to calibrate and set the cam reading to zero. Then, readings were made after each loading step.

3.4 Track loading

A load of 48.5-ton from a 4-axle Plasser tamping machine was applied to the track. The distance between two adjacent axles is 1.5 meters and between the two inside axles are 9.5 meters (Fig. 5). Therefore, the applied axle load is 12.15 tons on each axle. The tamping machine was run over the rail with the speed of zero, ten and twenty km/h.



Fig. 4. "Pull-Out" test instruments.

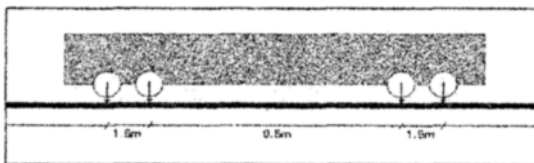


Fig. 5. Load applied to the track.

4. Field tests results

Results obtained from the load cells and the surveying cam were further analyzed using Excel program to draw and compare them graphically. They are presented as follows.

4.1 "Load-Cell" results

The speed of the tamping machine is increased in three steps. During the first step, static loading ($V_{loading}=0$) was applied to the track. The results are presented in Table 3 as well as Figs. 6 and 7.

During the second step the speed of the tamping machine was increased to 10 km/h. The results are presented in Table 4, and Figs. 8 and 9.

Table 3. Static-state recorded values in "Load-Cells".

Load Cell No.	1	2	3	4	5
Load Cell Reading Before Loading	4.98	1.45	1.43	0.85	0.51
Load Cell Reading After Loading	1.55	0.21	0.1	0.27	0.09
Absolute Value	3.43	1.24	1.33	0.58	0.42

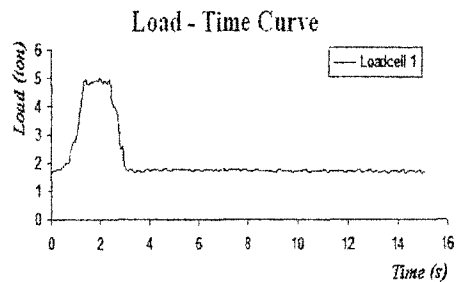


Fig. 6. Load vs. time in "Load-Cell" No.1 ($V_{loading}=0$).

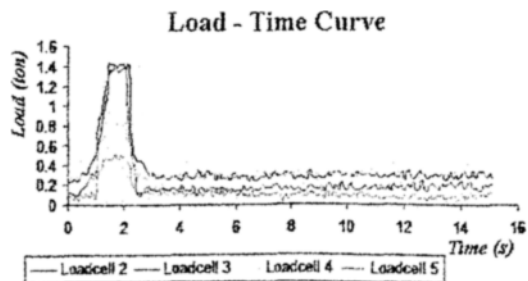


Fig. 7. Load vs. time in "Load-Cells" No. 2,3,4,5 ($V_{loading}=0$).

Table 4. Recorded values in "Load-Cells" $V_{loading}=10$ km/h, Axle load=12.15 ton, Wheel load=6.0625 ton.

Load Cell No.	1	2	3	4	5
Load Cell Reading Before Loading	5.47	1.58	1.72	1.05	1.042
Load Cell Reading After Loading	1.78	0.62	0.505	0.178	0.294
Absolute Value	3.69	0.96	1.215	0.872	0.748

Table 5. Recorded values in "Load-Cells" $V_{loading}=10$ km/h, Axle load=12.15 ton, Wheel load=6.0625 ton.

Load Cell No.	1	2	3	4	5
Load Cell Reading Before Loading	5.8	1.57	2.13	1.34	0.96
Load Cell Reading After Loading	2.25	0.49	0.67	0.41	0.346
Absolute Value	3.55	1.08	1.46	0.93	0.614

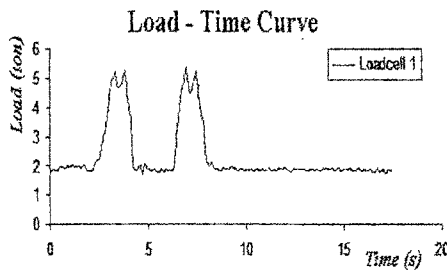


Fig. 8. Load vs. time in "Load-Cell" No.1 ($V_{loading}=10$ km/h).

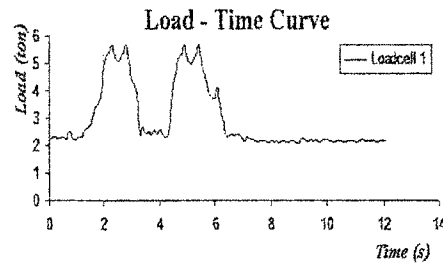


Fig. 10. Load vs. time in "Load-Cell" No.1 ($V_{loading}=20$ km/h).

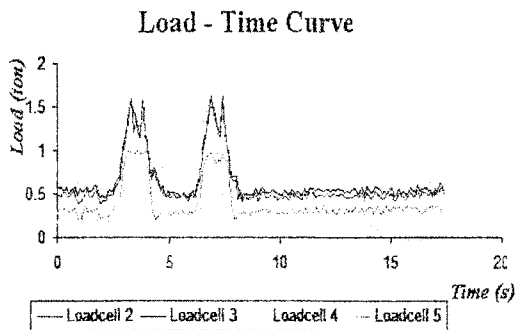


Fig. 9. Load vs. time in "Load-Cells" No. 2,3,4,5 ($V_{loading}=10$ km/h).

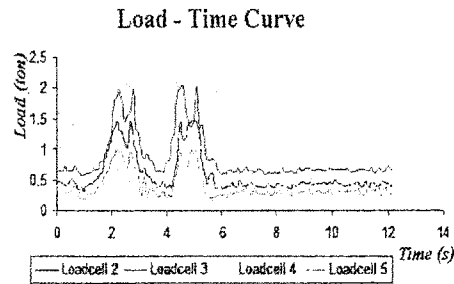


Fig. 11. Load vs. time in "Load-Cells" No. 2,3,4,5 ($V_{loading}=20$ km/h).

The test results recorded during the third test step ($V_{loading}=20$ km/h) are indicated in Table 5 as well as Figs. 10 and 11.

Due to the characteristics of the load cells, they were not set to zero before loading. Therefore, before loading and after removing the load, load cells show their initial values. In Tables 3 to 5, the second row is the load cell initial values (which are before loading or after removing the load), the third row is the load cell reading after loading, and the fourth row is the real value of the load transferred to the load cell which is obtained from the subtraction of the third row from the second row.

4.2 "Pull-Out" test results

The results obtained from the pull out test for the track with normal condition and the track right after the tamping operation are presented in Fig. 12.

4.3 Vertical rail deformation

Sleeper vertical deflections under the rail positions were measured. The load is as detailed in Section 3-4. The rail deflection on the top of the sleeper was measured when the load (the stabilizer machine) was located in eight different positions on the rail. Fig. 13 indicates the corresponding results for each loading condition. The vertical arrows in the Figs. represent the positions of the axles.

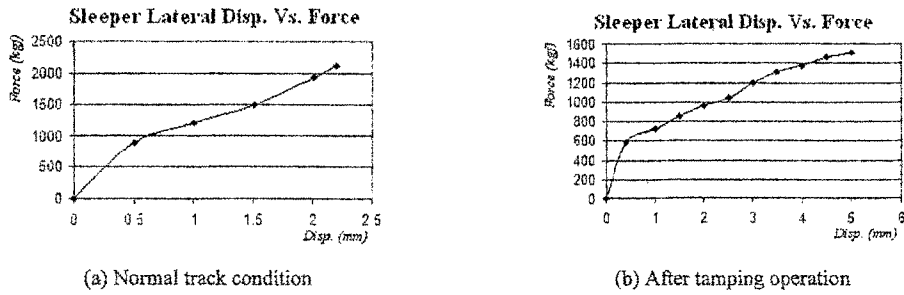


Fig. 12. "Pull-Out" tests results.

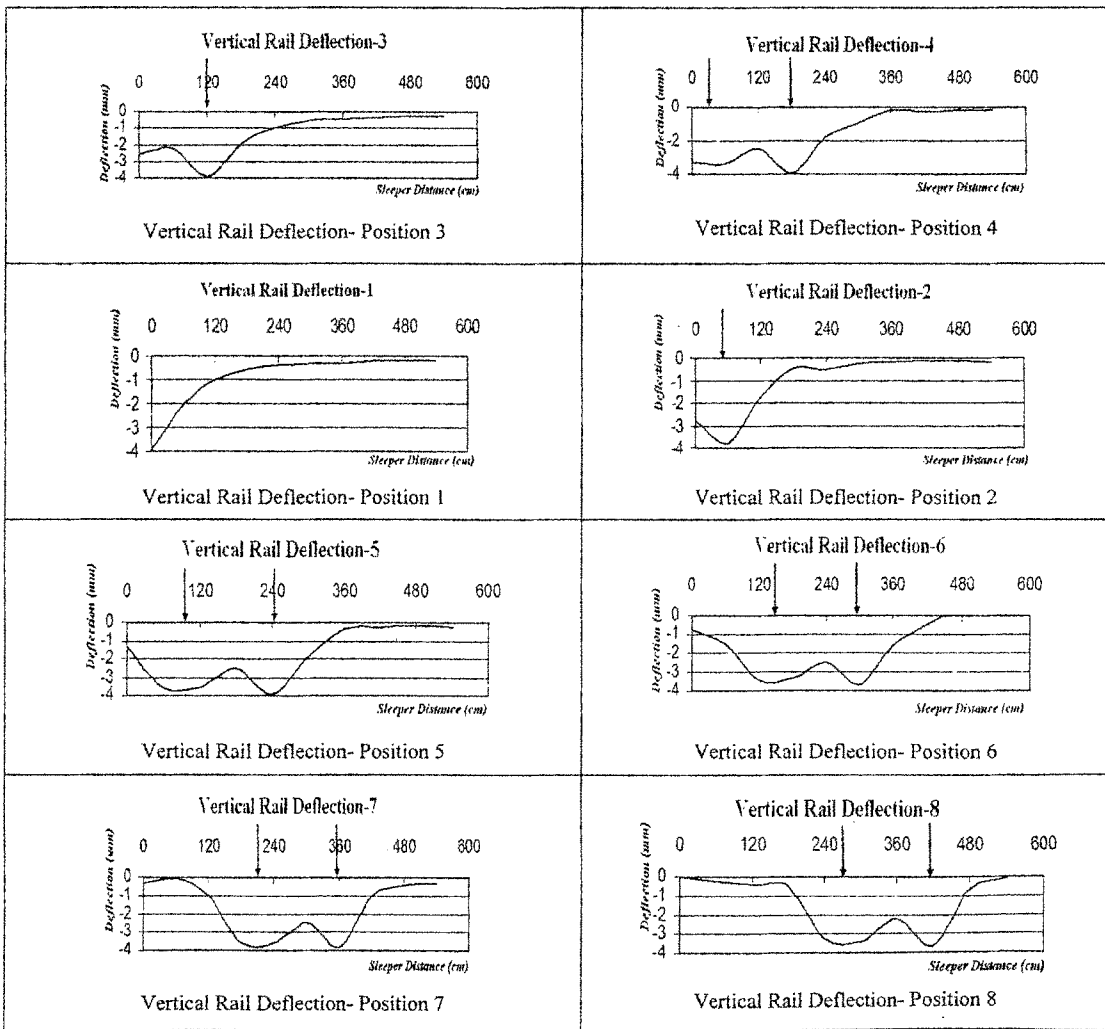


Fig. 13. Rail Vertical deformation results.

5. Discussions of the results

From the experimental results obtained in this research, several key sleeper analysis parameters can be studied. They include rail seat load, sleeper pressure

distribution under the sleeper, lateral resistance of concrete sleepers in the ballasted tracks, effect of tamping on the lateral resistance of the track, and rail deflections at the sleeper position.

Based on the results obtained, the ratio of the rail

seat load (q_r) to the wheel load (P) can be obtained as below.

$$(q_r)_{ave} = \frac{q_{r1} + q_{r2} + q_{r3}}{3} \tag{5}$$

$$\frac{q_r}{P} = \left(\frac{(q_r)_{ave}}{6.0625} \right) \tag{6}$$

Where $(q_r)_{ave}$ is the average of the rail seat load. q_{r1} , q_{r2} and q_{r3} are the rail seat loads obtained from the readings of the load cell positioned under the rail (load cell No.1) when the transient load (Fig. 5) is applied with the speed of zero, 10 and 20 km/h, respectively. According to Tables 3, 4, and 5, q_{r1} , q_{r2} and q_{r3} are 3.43, 3.69 and 3.55 (tons), respectively. Having the wheel load of 6.0625 (tons) and calculating $(q_r)_{ave}$, the ratio of the rail seat load to the wheel load becomes 0.59. That is, the maximum rail-seat load is equal to 59 percent of the wheel load. This agrees with what is suggested by AREMA [5]. On the other hand, the results are in contrast with the “three adjacent sleepers” theory which is mostly used by performance analysts.

The results obtained here do not confirm a uniform contact pressure between the ballast and the sleeper as suggested by AREMA [5]. They indicate a parabolic shape for the pressure distribution under the sleeper, having a maximum value at the rail positions with a symmetrical pattern. That is, the stress increases from the sleepers' edge and reaches its maximum value under the rail-seat position, then with a decreasing pattern, reaches its minimum value at the sleeper center. This pattern is compatible with the sleeper pressure distribution proposed by UIC [10] and Talbot [11] as they claim that sleeper pressure values follow a symmetrical half-sinusoidal shape. Fig. 14 presents a schematic view of the sleeper pressure distribution obtained in this research. This Fig. indicates that the speed of the transient load does not change the load distribution pattern although the amount of maximum and minimum pressures under the sleeper might be affected.

The results obtained from the pull-out test indicate a linear relationship between the lateral forces and the lateral movement of the sleeper. It should be noted that immediately after tamping, a noticeable reduction in the lateral resistance of the sleepers can be observed. This confirms the common practice of applying speed reduction after tamping operation. Table 6

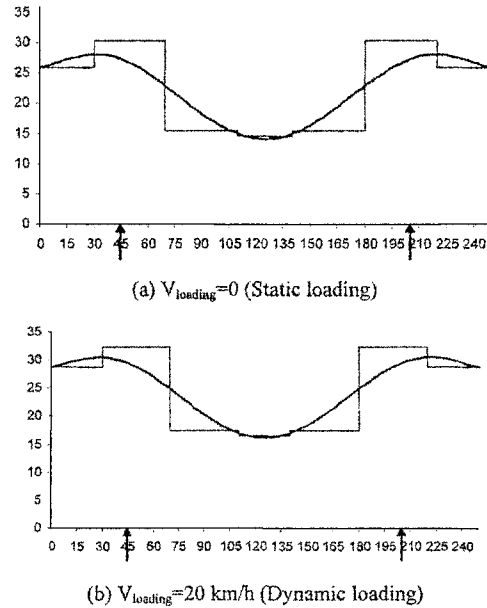


Fig. 14. Empirical sleeper pressure distribution obtained from field measurements.

Table 6. Measured sleeper lateral stiffness.

Condition	Stiffness (kgf/mm)
Normal Condition	660
Newly tamped track	300

indicates the sleepers lateral stiffness based on the measured data.

Taking into account the properties of the track components in the field, and using the Winkler model, the deflection of the rail-sleeper under the load (detailed in Fig. 5) was calculated. The theory of the pyramid model developed by Prause [12] was used for the calculation of the modulus of the foundation under the sleeper (k). A comparison between the results obtained here and those obtained from the Winkler model (the current practice) is presented in Fig. 15. This Fig. indicates some discrepancies between the results obtained from the field and those obtained from the Winkler model. The difference between the results is at the most 30%.

The maximum deflection which occurs under the wheel loads is about 27% higher than that obtained from the current practice. The simplicity of the Winkler model in use and the reasonable differences between the result obtained from the model and those obtained from the field justify the use of Winkler model in practice.

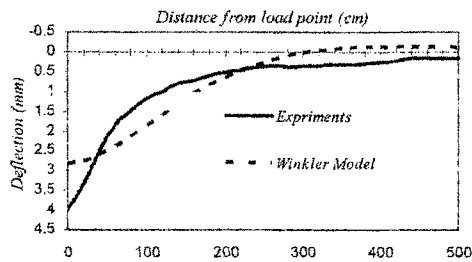


Fig. 15. Rail-sleeper deflection.

6. Conclusion

In this paper the results of a field investigation on the loading pattern of railway sleepers and the deflection of the sleepers under the rail are presented. Rail seat load, pressure distribution beneath the sleeper, lateral resistance of the sleepers in ballasted tracks, effect of tamping on lateral resistance of the track, and rail deflection at the sleeper position are investigated in this research.

The results obtained here confirm what is suggested by AREMA [5] for the calculation of the rail seat load. That is, the maximum rail-seat load is equal to 60 percentage of the wheel load. However, the results do not confirm a uniform contact pressure between the ballast and the sleeper as proposed by AREMA [5]. That is, the pressure between the ballast and the sleeper increases from the sleepers' edge and reaches its maximum value under the rail-seat position; then with a decreasing pattern, comes to the minimum value at the center of the sleeper. Results indicate that the same distribution pattern is obtained when dynamic loads are applied. This pattern is compatible with the recommended sleeper pressure distribution proposed by UIC [10] in which the sleeper pressure follows a symmetrical half-sinusoidal shape.

A linear relationship between the lateral forces and the lateral movement of the sleeper is obtained in this research. The results demonstrate that track tamping reduces the lateral resistance of the sleeper by half. The results obtained for the deflection of the rail at the sleeper positions indicate some discrepancies between the rail deflections obtained in the field and those obtained from the Winkler model. The maximum deflection which occurs under the wheel loads at the sleeper positions is about 27% higher than the rail deflections obtained from the current practice. Due to the simplicity of the Winkler model in practice and the reasonable amount of errors obtained when applying this model, the use of this model in practice

seems to be justifiable.

For the continuation of this research work and further improvement of the current understanding of the behavior of sleepers, the implementation of a long-term testing approach in different loading conditions is recommended. Research in this area is in progress.

References

- [1] A. D. Kerr, *Fundamentals of Railway Track Engineering*, Simmons-Boardman Books, Inc., (2003) 66-89.
- [2] J. Sadeghi, Investigation on the accuracy of current practices in analysis of railway track sleepers, *International Journal of Civil Engineering*, 3 (1) (2005) 34-51.
- [3] J. A. Zakeri, J. Sadeghi., Field investigation of behavior of sleepers under moving loads, Final Research Reports submitted to the Department of Railway Engineering, MRT, No. rte543. Tehran, Iran. (2006).
- [4] S. L. Grassie, Dynamic modeling of railway track and wheel sets, invited paper, Second International Conference on Recent Advances in Structural Dynamics, University of Southampton, (1984).
- [5] AREMA, *Manual for Railway Engineering*, American Railway Engineering and Maintenance Way Association, Chapter. 5 and Chapter 30, Part.1, (2006) 11-17.
- [6] J. S. Mundrey, *Railway Track Engineering*, McGraw-Hill, New Delhi, (2003).
- [7] S. Chrismer and E. T. Selig, , Computer model for ballast maintenance planning, 5th International Heavy Haul Railway Conference, (1993) 223-227.
- [8] J. Sadeghi and B. Akbari, Field investigation on effects of railway track geometry parameters on rail wears, *International Journal of Zhejiang University, Science A*, 7 (11) (2006) 1846-1855.
- [9] M. Hetenyi, *Beams on an elastic foundation*, The University of Michigan Press, Ann Arbor, MI, (1946) 45-73.
- [10] IC Leaflets, UIC 861-1 O, Technical specification for the supply of non-treated track support (sleepers for standard and broad-gauge track and crossing), (2005).
- [11] A. N. Talbot, Stresses in Railroad Track, report of the special committee on stresses in railroad track, *Proceeding of AREA*, Six progressive Report, AREA proceeding, 45 (1933) 68-848.
- [12] R. H. Prause, H. C. Meacham, assessments of design tools criteria for urban rail track structure, vol. 1, A-Grade-Ballast Track, Battelle Columbus Laboratories, UMTA Report No. UMA-06-0025-74-4, National Technical Information Service, US Department of Commerce, Springfield, Virginia. (1974).